Scientific Journal of Silesian University of Technology. Series Transport
Zeszyty Naukowe Politechniki Śląskiej. Seria Transport

Volume 131 **2026**

p-ISSN: 0209-3324

e-ISSN: 2450-1549

DOI: https://doi.org/10.20858/sjsutst.2026.131.15

Journal homepage: http://sjsutst.polsl.pl

Article citation information:
Warczek, J., Gąszczak, A. Analysis of procedures for adapting the technical parameters of a propeller drive with an electric motor – a case study. *Scientific Journal of Silesian University of Technology. Series Transport*. 2026, **131**, 253-273. ISSN: 0209-3324.
DOI: https://doi.org/10.20858/sjsutst.2026.131.15

Jan WARCZEK[1], Aleksander GĄSZCZAK[2]

ANALYSIS OF PROCEDURES FOR ADAPTING THE TECHNICAL PARAMETERS OF A PROPELLER DRIVE WITH AN ELECTRIC MOTOR – A CASE STUDY

Summary. Selecting a propeller for a non-standard powerplant poses a significant challenge in aircraft design, particularly when engine parameters deviate from conventional aviation standards. This paper presents a methodology for assessing the compatibility of a three-blade Clark-Y airfoil propeller with selected propulsion configurations using aerodynamic and computational relationships. The approach enables verification of its applicability in non-standard design cases and supports flexible implementation across diverse propulsion systems. The method, its application, and potential use in engine-propeller integration are presented.
Keywords: propeller, electric propulsion, propeller selection, aerodynamic analysis

1. INTRODUCTION

The selection of a propeller for a propulsion unit constitutes a complex problem in which the engine characteristics define the admissible operating points, while the geometry and

[1] Faculty of Transport and Aviation Engineering, The Silesian University of Technology, Krasińskiego 8 Street, 40-019 Katowice, Poland. Email: jan.warczek@polsl.pl. ORCID: https://orcid.org/0000-0002-4767-5588
[2] Faculty of Transport and Aviation Engineering, The Silesian University of Technology, Krasińskiego 8 Street, 40-019 Katowice, Poland. Email: olekgaszczak@gmail.com. ORCID: https://orcid.org/0009-0006-5308-537X

settings of the propeller determine the power absorption, generated thrust, and efficiency as a function of forward velocity. These relationships may be described analytically using classical theoretical approaches based on momentum theory, blade element theory, and their extensions in the form of combined methods and vortex models [2, 9, 14]. These approaches form the foundation of both design and application calculations, enabling a quantitative assessment of the influence of geometric parameters and operating conditions on propeller characteristics.

The parameterization of propeller geometry, including diameter, number of blades, twist, and aerodynamic profile, has a direct impact on the load distribution and efficiency within a given range of advance ratio [6, 10]. The properties of aerodynamic airfoils, commonly used in aviation, remain an essential element of modeling both in classical approaches and in the interpretation of numerical calculation results. On this basis, numerous design procedures have been developed in which blade geometry constitutes the primary decision variable [1].

A significant portion of existing methods focuses on the design or optimization of propeller geometry, where the distribution of twist and chord along the blade is selected to maximize efficiency or satisfy a specified energy criterion at a given operating point [10, 11, 17, 25]. These approaches are sometimes extended to include specific conditions, such as operation at high altitude or in environments with reduced air density, characteristic of high-altitude and stratospheric platforms [20, 21]. In such cases, the propeller geometry is strictly subordinated to defined operating conditions, and the operating point is treated as a design element.

In real applications, however, propeller operating conditions deviate from ideal assumptions. Performance characteristics are influenced by aerodynamic interactions, including the interaction of the propeller slipstream with the wing or fuselage, the cooperation of multiple propellers, and unsteady flow conditions in multirotor systems [15, 19, 22]. Changes in effective inflow velocity and load distribution lead to significant differences between characteristics calculated for an isolated propeller and those observed under real operating conditions [16]. Additionally, acoustic and diagnostic aspects are analyzed, indicating the multidimensional nature of propeller selection criteria in engineering practice [17, 18].

Classical propeller selection procedures were developed primarily with respect to internal combustion engines. Analyzes concerning fixed-pitch propellers for low-power units organize the relationships between shaft power, rotational speed, and the selection of diameter and pitch, while also indicating limitations resulting from engine characteristics [6, 7]. This issue also appears in multirotor applications with internal combustion propulsion, where it affects the stability and efficiency of the entire system [12].

In the case of electric propulsion systems, the emphasis shifts toward different constraints. The characteristics of electric motors, including parameters such as efficiency, torque limitations, and maximum rotational speed, combined with the properties of controllers and energy sources, determine the range of achievable propeller operating points [8, 13, 23]. Analyzes conducted for small electric aircraft, UAV platforms, and VTOL configurations show that propeller selection is a compromise and involves the simultaneous evaluation of thrust, efficiency, and power margin across different phases of flight [3, 4, 5]. In this context, selection procedures based on available propeller and motor characteristics are being developed, without the need to design a new blade geometry [5, 13].

The above considerations lead to a clear distinction between propeller geometry design and the selection of operating parameters for a propeller with known geometric characteristics. In many design applications, the problem reduces to determining rotational speed and blade setting angle and consequently selecting the range of advance ratio and propeller efficiency, for a given number of blades with specified aerodynamic profiles and diameter, taking into account the known characteristics of the propulsion unit [2, 9, 7]. Iterative procedures developed for electric propulsion systems also exist, linking propeller selection with the motor, controller, and energy source, focusing on the evaluation of achievable operating points and power balance [23, 24]. In parallel, formal multi-criteria selection approaches are being developed, in which relationships between thrust, efficiency, and power consumption are analyzed, while emphasizing the importance of low computational cost methods in parametric analyses [17, 24, 25].

In this study, assumptions were adopted in which the starting point consists of the characteristics of the propulsion unit considered for an electric motor and a propeller with defined geometry. The subject of the developed method is a sequential procedure for determining propeller operating parameters, in particular rotational speed and overall blade geometry, enabling a comparable assessment of the matching between the engine and propeller without transitioning into the design of a new blade geometry. The aim of the study is to develop a universal, algorithmic procedure for selecting a propeller for a propulsion unit, enabling the determination of propeller operating parameters for a given geometry and specified operating conditions.

The study adopts an approach in which the characteristics of the propulsion unit constitute the input data, and the computational process leads to the determination of the working propeller diameter, blade setting angle, and operating points of the engine-propeller system.

The developed procedure was used to determine the design features of the selected engine-propeller assembly. Its advantage is the ability to select the parameters of any drive unit, allowing for its potential application to both electric motors and combustion engines with non-standard external characteristics (rotary piston engines).

2. TECHNICAL ASSUMPTIONS AND PROPULSION SYSTEM PARAMETERS

The algorithmic propeller selection process is based on clearly defined input assumptions resulting from the properties of the propulsion unit and the operating conditions of the aircraft. The preliminary algorithm presented in Fig. 1 does not assume a specific type of propulsion or propeller configuration but uses engine characteristics and flight parameters as input data for subsequent stages of the propeller propulsion system design process.

2.1. Selection of propulsion system configuration

The starting point is the selection of the propulsion unit and the propulsion system configuration. At this stage, the external characteristics of the engine are analyzed in the form of torque and power curves as a function of rotational speed, which define the available operating range of the propeller-engine system and the level of power that can be transmitted to the propeller.

The propeller-engine system is analyzed in relation to a specific aircraft, which requires the adoption of basic operating conditions such as cruise speed and flight altitude. On this basis, the target propeller's rotational speed is determined, considering engine characteristics and aerodynamic limitations. If necessary, the gear reduction ratio is also determined to ensure compatibility between the operating ranges of the engine and the propeller. The adopted assumptions allow the same propeller selection procedure to be applied to different types of propulsion units.

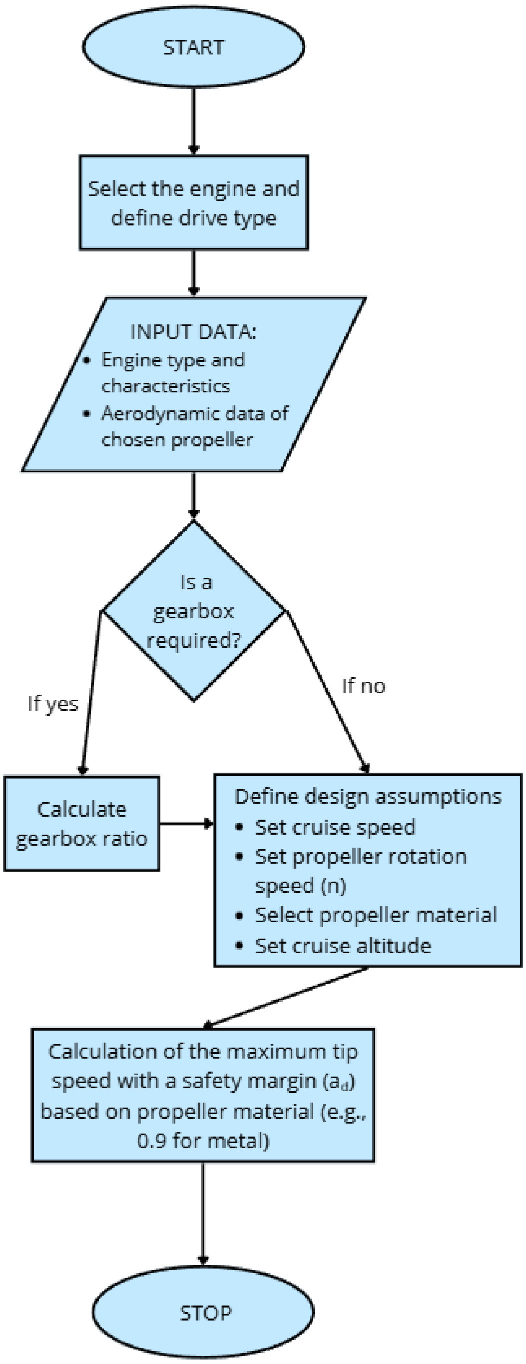

Fig. 1. Diagram of the preliminary process of selecting the propulsion unit and propulsion system configuration

2.2. Example engine characteristics

Electric propulsion systems in aviation constitute one of the most dynamically developing directions of modern engineering. The use of electric motors allows for a significant reduction in noise emissions as well as simplification of propulsion system design. Despite significant limitations related to battery energy density, the development of energy storage technologies and hybrid systems indicates a growing potential for the application of electric propulsion, particularly in light aviation, regional aviation, and unmanned aerial vehicles. There are already available design solutions for electric motors optimized for aviation applications, such as the EMRAX 348. This electric motor exhibits characteristics typical of electric propulsion systems as shown in Fig. 2, where high torque is available already at low rotational speeds, and the torque curve as a function of speed is significantly flatter. The motor power increases with rotational speed until the rated value is reached, after which it remains at a similar level over a wide range of speeds. In practice, this enables direct coupling of the motor with the propeller or the use of a gearbox with a significantly lower reduction ratio compared to an internal combustion engine.

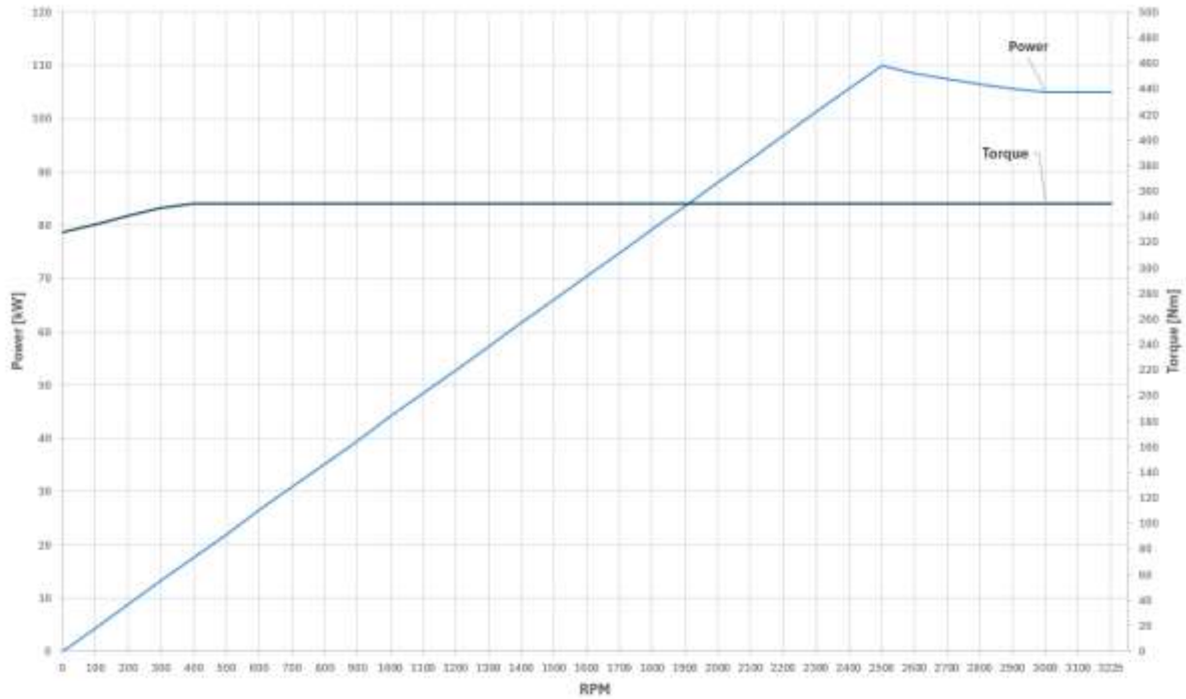

Fig. 2. External characteristics of the EMRAX 348 electric motor [11]

2.3 Aerodynamic analysis of an example propeller

The aerodynamic analysis was carried out for a three-bladed propeller with a Clark Y airfoil, adopted as the reference profile shown in Fig. 3, with well-documented aerodynamic properties. At this stage, the propeller is treated as an object with a defined geometry, and the purpose of the analysis is to describe the mechanism of airflow interaction with the blade and the resulting distribution of aerodynamic forces under different flight conditions.

The fundamental element of the aerodynamic description of the blade is its cross-section, whose geometry is defined by the airfoil shape and the chord length c. The orientation of the chord relative to the plane of propeller rotation is determined by the angle θ, understood as the blade setting angle. The value of this angle, combined with the local direction of the incoming airflow, defines the angle of attack α.

An elementary blade section is subjected to the local flow velocity V_s, which is the resultant of the tangential velocity V_{tip}, resulting from the rotational motion of the propeller, and the axial inflow velocity V_∞, associated with the forward motion of the aircraft. The result of these components determines the local inflow direction and its angle relative to the airfoil chord c.

This relationship determines both the magnitude of the generated aerodynamic forces and their spatial distribution.

a) b)

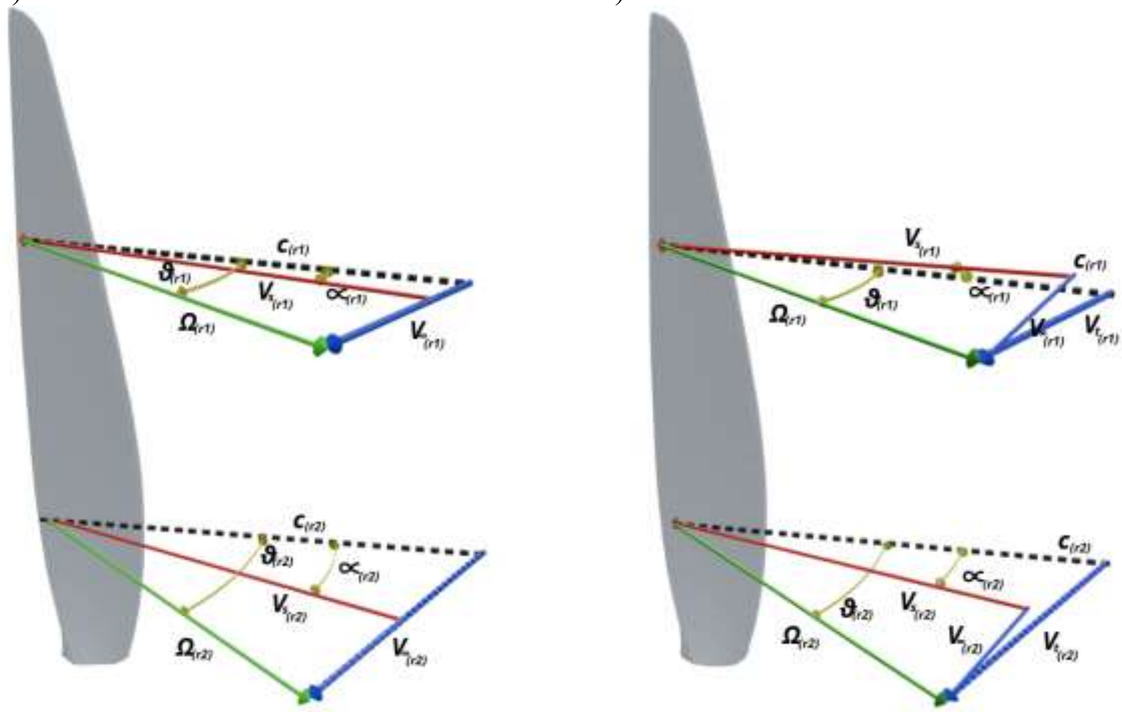

Fig. 3. Analysis of velocity vectors and aerodynamic angles of a propeller blade in straight flight and during altitude change

In the case of straight flight, the inflow velocity has a fixed axial direction, consistent with the direction of motion of the aircraft. The tangential velocity vector V_{tip}, resulting from the angular velocity of the propeller, remains perpendicular to the blade radius R, and the resultant of both components forms a stable system of local velocity vectors. For a given angle θ, this leads to a uniquely defined aerodynamic angle of attack α of the airfoil at a given blade radius. Under these conditions, the generated aerodynamic force can be decomposed into an axial component, responsible for generating thrust T, and a tangential component, generating a resistive torque opposing the rotational motion of the propeller. The distribution of these forces along the blade radius is ordered and serves as a reference point for further analysis.

In the case of flight with a trajectory different from the direction of the airflow inflow, for example during climb, both the magnitude and direction of the axial component of the inflow velocity change. As a result, the local inflow direction on the blade differs from the straight flight case, which leads to a change in the resultant flow velocity V_s and a modification of the local angle of attack α. This change is clearly visible in the three-dimensional representation of velocity vectors and aerodynamic forces, where a different orientation of the resultant velocity and the corresponding component of the aerodynamic force is observed. Consequently, the proportion of the axial and tangential force components changes, which affects both the value of the generated thrust T and the resistive torque acting on the propeller.

Such a separation of the analysis into the case of straight flight and flight with a modified inflow direction allows for an unambiguous interpretation of the influence of flight conditions on the local angle of attack α and the distribution of aerodynamic forces on the blade.

The visualization of these relationships provides a clear extension of classical two-dimensional schemes and forms a coherent introduction to further quantitative analysis of propeller operation.

2.4 Kinematic constraints and propeller operating conditions

Based on the defined input parameters and the adopted aerodynamic model of the propeller, additional constraints are introduced, resulting directly from the operating conditions of the propulsion system. One of the key constraints is the maximum allowable linear speed of the blade tip V_{ad}, referenced to the local speed of sound. This limitation arises from the need to avoid wave phenomena, a rapid increase in aerodynamic drag, and unfavorable dynamic loads acting on the blade.

In order to account for these effects in the algorithm, a safety margin dependent on the propeller material was adopted. For the analyzed metal propeller, it was assumed that the maximum blade tip speed does not exceed 90% of the local speed of sound. The adoption of such a margin allows for maintaining safe operating conditions of the propeller over the entire considered range of rotational speeds.

Based on the velocity V_{ad} and the prescribed rotational speed of the propeller, the maximum allowable propeller diameter D_{max} is determined according to relation (1). This limitation is kinematic in nature and constitutes an upper geometric bound, independent of further aerodynamic and performance analyzes.

$$D_{max} = \frac{2}{2\pi \cdot RPS}\sqrt{(V_{ad}^2) - (V^2)}\ [m] \tag{1}$$

where:
RPS – propeller rotational speed [1/s],
V_{ad} – maximum propeller speed defined by safety factor [m/s],
V – flight speed [m/s].

The D_{max} determined in this way constitutes one of the fundamental assumptions for further calculations and defines the range within which propeller geometric variants are analyzed. Only in the next stage is it possible to relate this limitation to the geometric characteristics of the propeller and to evaluate its efficiency as a function of flight conditions and the propulsion unit.

3. DETERMINATION OF GEOMETRIC AND AERODYNAMIC PROPELLER PARAMETERS

Based on the characteristics of the propulsion unit, flight conditions, and the kinematic limitation of the propeller, it is possible to determine the preliminary working diameter of the propeller. This stage, presented in the block diagram shown in Fig. 4, is based solely on the parameters and assumptions adopted earlier and constitutes their direct computational consequence.

The basis for further analysis consists of dimensionless parameters describing propeller operation, particularly the advance ratio J defined by equation (2) and the power coefficient C_p defined by relation (3). The advance ratio J is defined as the forward distance traveled by the aircraft during one revolution of the propeller and results directly from the assumed flight speed and propeller rotational speed. The power coefficient C_p expresses the power requirement of the propeller in relation to its diameter, rotational speed, and air density, and is calculated based on the power available from the propulsion unit and the assumed flight conditions. The values of both parameters are not selected but follow directly from the previously adopted assumptions.

$$J = \frac{V}{RPS \cdot D} \tag{2}$$

where:
RPS – propeller rotational speed [1/s],
D – propeller diameter [m],
V – flight speed [m/s].

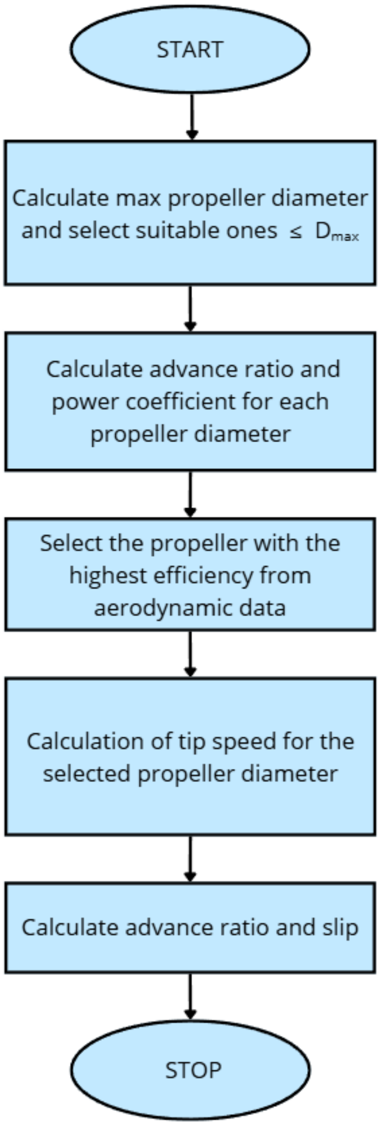

Fig. 4. Diagram of the process of selecting the propeller diameter and blade setting angle θ for a selected propulsion unit

$$C_p = \frac{P_p}{\rho \cdot RPS^3 \cdot D^5} \tag{3}$$

where:
P_p – power absorbed by the propeller [W],
ρ – air density [kg/m^3],
D – propeller diameter [m],
RPS – propeller rotational speed [1/s].

3.1. Propeller geometric parameters – analysis of possible solutions

In the first step, a set of working diameters D_i smaller than the previously determined limit value D_{max} is considered. For each analyzed diameter D_i, with unchanged assumptions regarding flight speed V, propeller rotational speed Ω, and propulsion unit power P, the corresponding values of advance ratio J and power coefficient C_p are determined. These values are then plotted on the power coefficient versus advance ratio chart shown in Fig. 5, containing families of curves corresponding to different values of the geometric blade setting angle θ. On this basis, the blade setting angle is determined at which the propeller power requirement matches the power available from the propulsion unit for a given diameter.

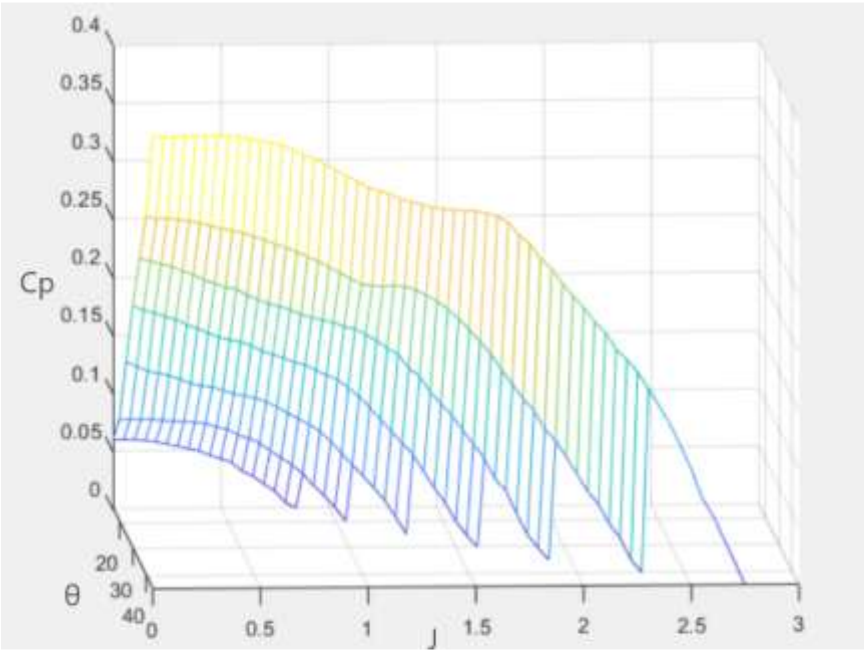

Fig. 5. Power coefficient characteristics of a three-bladed propeller with a Clark Y airfoil

After determining the angles θ for the given diameters D_i, an evaluation of the propeller efficiency η_p is carried out. For this purpose, the calculated values of the advance ratio J are correlated with propeller efficiencies, as shown in Fig. 6. Then, the curve corresponding to the determined angle θ is selected, and on this basis, the efficiency η_p is determined for successive propeller diameters D_i. The procedure is repeated for all considered diameters, and the selection of the working diameter is made based on the obtained efficiency values η_p as the solution ensuring the highest aerodynamic efficiency under the assumed conditions.

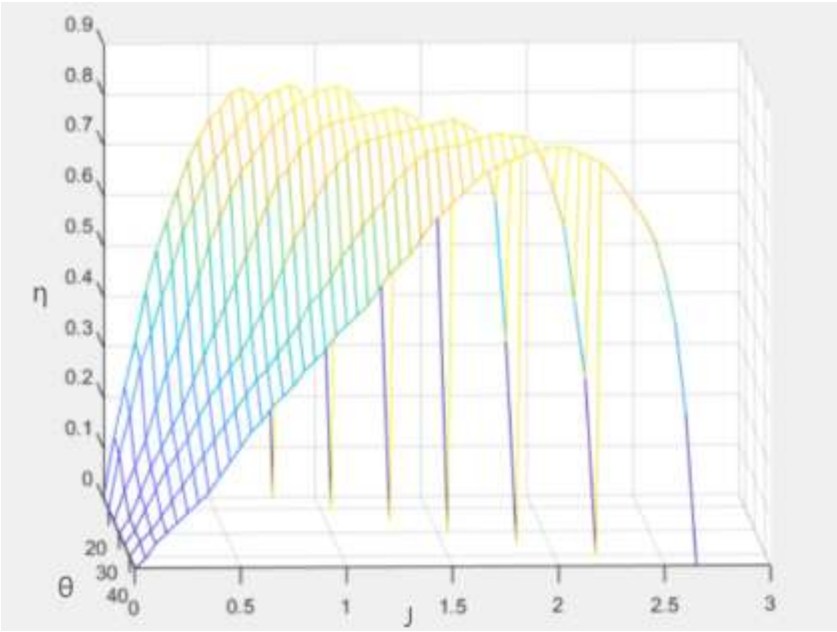

Fig. 6. Efficiency characteristics of a three-bladed propeller with a Clark Y airfoil

3.2. Verification of propeller diameter selection

After determining the propeller diameter, it is possible to verify the obtained solution with respect to the assumptions adopted in earlier stages of the algorithm as shown in equation (4). First, the linear speed of the blade tip V_{tip} is calculated for the diameter D_i and the given propeller rotational speed. The obtained value is compared with the allowable blade tip speed V_{ad}, resulting from the adopted safety margin, which allows for an unambiguous assessment of compliance with kinematic constraints.

$$V_{tip} = \sqrt{V^2 + (\pi \cdot RPS \cdot D)^2} \quad [\frac{m}{s}] \tag{4}$$

where:
V – flight speed [m/s],
RPS – propeller rotational speed [1/s],
D – propeller diameter [m].

In parallel, it is possible to determine the propeller slip s, understood as the difference between the geometric pitch H_g and the aerodynamic pitch H_a. The geometric pitch H_g results directly from the propeller geometry and the selected angle θ, while H_a is determined based on the actual forward velocity of the aircraft and the propeller rotational speed, as shown in equations (5) and (6). The slip s represents a measure of losses resulting from aerodynamic interactions and allows for the assessment of the degree of utilization of the propeller's potential under given flight conditions as defined by equation (7).

$$H_g = 2 \cdot \pi R \cdot tg\theta \quad [m] \tag{5}$$

where:
R – propeller radius [m],
θ – blade setting angle [deg].

$$H_a = \frac{V}{RPS} \quad [m] \tag{6}$$

where:
RPS – propeller rotational speed [1/s],
V – flight speed [m/s].

$$s = \frac{H_g - H_a}{H_g} \cdot 100 \quad [\%] \tag{7}$$

where:
H_a – aerodynamic pitch [m],
H_g – geometric pitch [m].

The determination of V_{tip} and the slip s constitutes the final stage of verifying the correctness of the selected diameter D_i. Meeting the kinematic constraints and obtaining an acceptable slip value confirm that the selected solution is consistent with the assumptions of the algorithm and may be adopted as a correct configuration of the engine-propeller system for further work. After determining the propeller's diameter and the preliminary operating parameters, it is possible to proceed to the analysis of the cooperation between the propeller and the propulsion unit under flight conditions.

Based on the determination of the actual operating points of the propeller-engine system and their subsequent evaluation in terms of aerodynamic efficiency and operational economy, an analytical coupling of the propeller and propulsion unit characteristics is performed. This enables a transition from geometric analysis to operational analysis, as shown in the block diagram Fig. 7.

The next step is to determine the operating points of the engine-propeller system. The analysis is carried out as a function of the propulsion unit at rotational speed Ω. A discrete set of rotational speeds is considered, covering the significant operating range of the engine. For each rotational speed, the power delivered by engine P is known, resulting directly from its characteristics. On this basis, for each value of rotational speed, the propeller power coefficient C_p corresponding to the current operating conditions is calculated according to equation (8).

$$C_p = \frac{M_p}{\rho \cdot RPS^2 \cdot D^5} \tag{8}$$

where:
M_p – torque on the motor shaft [Nm],
ρ – air density [kg/m^3],
D – propeller diameter [m],
RPS – propeller rotational speed [1/s].

Then, using the geometric characteristics of the analyzed propeller and the previously determined blade setting angle θ, the corresponding value of the advance ratio J is determined for each value of C_p. The analysis is carried out based on the characteristics of the relationship between the power coefficient and the advance ratio for a constant value of the angle θ, which ensures consistency of calculations over the entire analyzed range of rotational speeds.

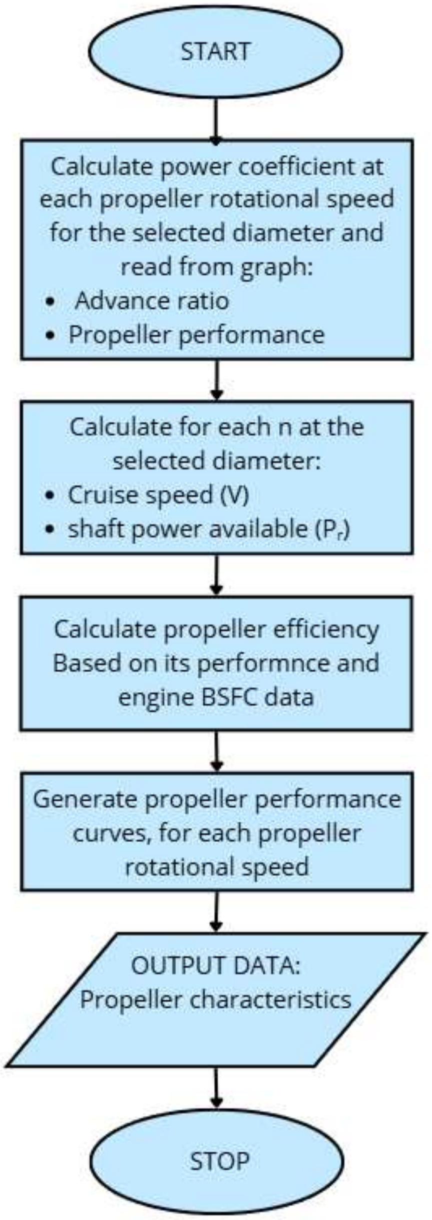

Fig. 7. Diagram of the procedure for determining the characteristics of the engine-propeller propulsion system

After determining J, the propeller efficiency η_p is determined. For a given value of J and the same angle θ, efficiency characteristics are used, from which the corresponding value of η_p is read. As a result, for each operating point, a set of data is obtained including rotational speed, engine power, power coefficient, advance ratio, and efficiency.

Based on the advance ratio, rotational speed, and propeller diameter, the corresponding flight speed and rated power are calculated equations (9) and (10). In this way, a table of operating points of the propeller-engine system is created in Tab. 1, forming the basis for further analysis.

$$V = RPS \cdot J \cdot D \ [\frac{m}{s}] \tag{9}$$

where:
J – advance ratio,
D – propeller diameter [m],
RPS – propeller rotational speed [1/s].

$$P_r = P_p \cdot \eta_p \quad [W] \tag{10}$$

where:
P_p – power absorbed by the propeller [W],
η_p – propeller efficiency.

Tab. 1

Operating points of the engine-propeller propulsion system
as a function of propeller rotational speed

RPS	P [W]	C_p	J	η [%]	V [m/s]	P_r [kW]	V [km/h]
54	105000	0,031	0,9	**83**	91,37	87,15	328,9248
52	105000	0,035	0,88	**83,5**	86,03	87,675	309,70368
50	105000	0,039	0,86	**84**	80,84	88,2	291,024
48	106000	0,045	0,8	**83**	72,19	87,98	259,8912
46	107000	0,051	0,79	**82,5**	68,32	88,275	245,94912
44	109000	0,060	0,72	**82**	59,56	89,38	214,41024
42	110000	0,070	0,65	78	51,32	85,8	184,7664
40	104760	0,077	0,58	72	43,62	75,4272	157,0176
38	99520	0,085	0,35	55	25,00	54,736	90,0144

3.3. Criteria for selecting the operating point of the engine-propeller system

The obtained table of operating points makes it possible to take into account the criterion of operational efficiency of the propulsion unit. Selecting the point with the highest propeller efficiency alone does not always lead to the most favorable operating conditions; therefore, it is necessary to relate the results to the energy characteristics of the engine.

In the case of an internal combustion engine, the analysis would be carried out based on brake specific fuel consumption (BSFC) maps, allowing identification of the range of rotational speeds and loads characterized by minimal fuel consumption. For an electric motor, an analogous criterion is formulated based on motor efficiency maps, enabling the identification of the range of rotational speeds at which energy conversion efficiency reaches its maximum values presented in Fig. 8.

Among the operating points determined in Tab. 1, those that fall within the range of rotational speeds favorable from the perspective of energy consumption are preferred. In the case of a discrepancy between maximum propeller efficiency and minimum energy consumption, the selection of the operating point constitutes a compromise, with priority given to the criterion of the operational economy.

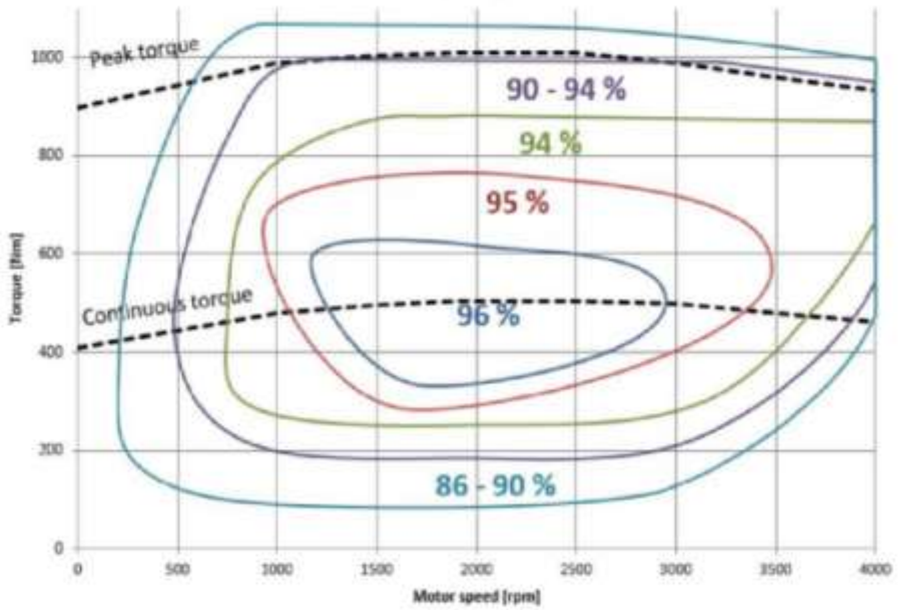

Fig. 8. Efficiency map of the EMRAX 348 electric motor as a function of rotational speed and torque [11]

4. DETERMINATION OF PROPELLER GEOMETRY

Based on the results of the propeller selection algorithm, a geometric model was developed, constituting a spatial representation of the obtained parameters. This model was created based on a known reference geometry, appropriately scaled to the diameter resulting from the calculations. Its purpose is to present the resulting propeller geometry and to enable its further analysis in both geometric and aerodynamic terms.

The three-dimensional propeller model reflects the distribution of blade geometry along the radius, resulting directly from the applied algorithm. The use of the Clark Y aerodynamic profile and the determined distribution of angles of attack allows validation of the obtained geometry with the adopted aerodynamic assumptions. The model enables analysis of the continuity of blade setting changes and the relationship between geometry and the operating conditions of the propeller-engine system. The developed geometric form represents the physical outcome of the algorithm and allows assessment of its correctness in the context of the actual propeller design, as shown in Fig. 9. The model thus serves as an interpretative tool, linking computational results with their spatial representation.

For the analysis of local aerodynamic properties of the blade, working sections were applied, determined in a manner corresponding to the actual operating conditions of the propeller in rotational motion. These sections were obtained by defining the blade geometry on the surface of a cylinder coaxial with the axis of propeller rotation and then unwrapping the resulting section onto a plane, as shown in Fig. 10. The aerodynamic section defined in this way corresponds to V_s and enables analysis of the working airfoil under conditions resulting from rotational motion.

Fig. 9. Geometric model of the designed propeller for the analyzed engine-propeller propulsion system

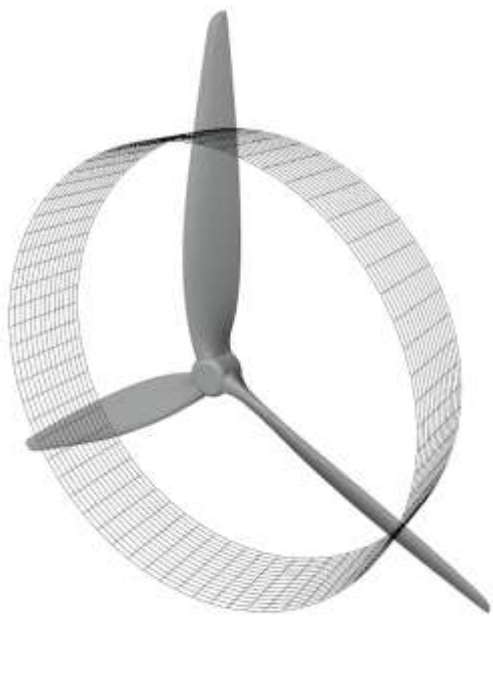

Fig. 10. Example surface of motion of flow particles around the blade at a given radius *R=0.75*

Example sections were created for selected propeller radii: *R=0.3*, *R=0.55*, and *R=0.75*, which allows for the assessment of changes in airfoil shape along the radius and their relationship with the distribution of aerodynamic load. These sections represent the local working airfoils of the blade at the indicated radius, as shown in Fig. 11.

The analysis of the sections allows for a qualitative assessment of the influence of blade setting distribution on the airfoil shape and its orientation relative to the local flow velocity V_s. Particular attention was given to the section at radius *R=0.75*, which in the propeller selection algorithm serves as the reference point for determining the blade setting angle θ.

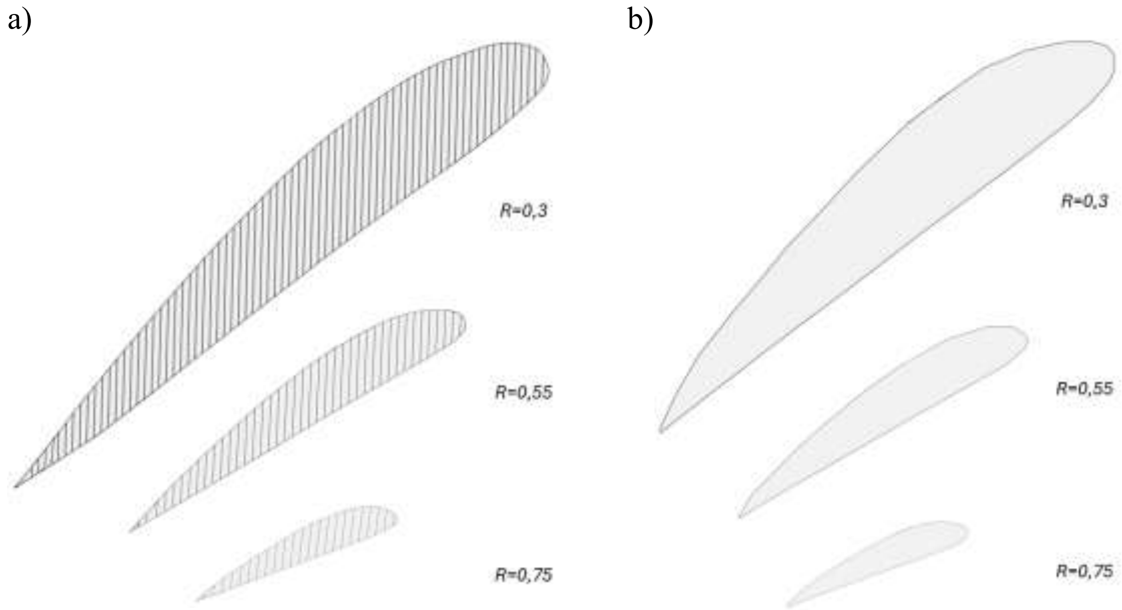

Fig. 11. Comparison of aerodynamic and geometric blade sections at radius R=0.3, R=0.55, and R=0.75

The presented sections allow for a direct correlation between the results of the algorithm and the local aerodynamic properties of the blade and constitute an important element in the interpretation of the obtained results. However, it should be emphasized that the chords determined for the aerodynamic airfoil are longer than the corresponding chords of the geometric airfoil, and the scale of this difference varies along the blade radius. In the conducted analysis, it was found that for the section located at the relative radius *R=0.3*, the chord extension is approximately 14.0%, for the section at *R=0.55* approximately 14.9%, and for the section at *R=0.75* approximately 16.3%. This is the result of the nonlinear mapping of the section on a rotational surface and its unwrapping into a flat form, because of which this difference does not have a constant value along the entire blade length. Taking this effect into account is significant in the interpretation of section geometry and in further analysis of the aerodynamic properties of the propeller.

5. ANALYSIS OF THE ENGINE-PROPELLER SYSTEM AS A FUNCTION OF PROPELLER ROTATIONAL SPEED

Based on the selected operating points, it is possible to develop characteristics of the propeller-engine system as a function of propeller rotational speed *RPS*. The propeller rotational speed serves as the independent variable, enabling a consistent comparison of propulsion system operating parameters. It is possible to define the relationship between flight speed and rotational speed *RPS*, as shown in Fig. 12. The characteristics of available power P_r presented in Fig. 13 and efficiency η_p shown in Fig. 14 are then determined.

These characteristics allow for the evaluation of the behavior of the propeller-engine system within the analyzed operational range and provide a basis for comparing results obtained for different types of propulsion units.

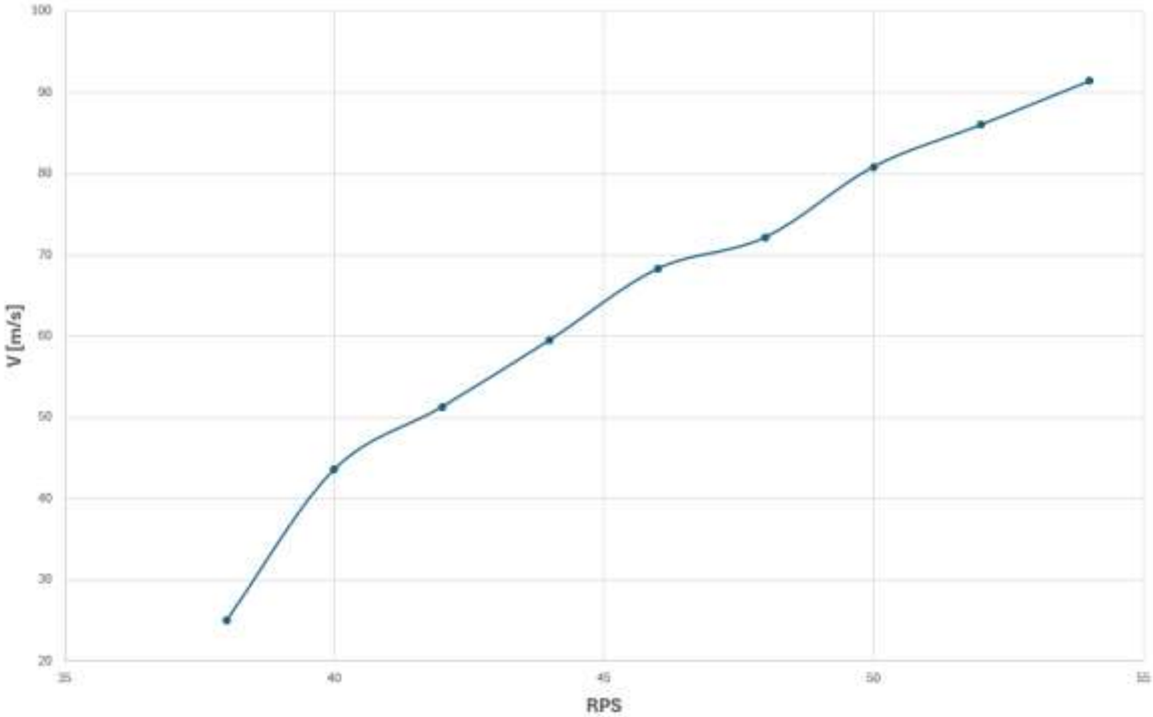

Fig. 12. Variation of aircraft forward speed as a function of propeller rotational speed

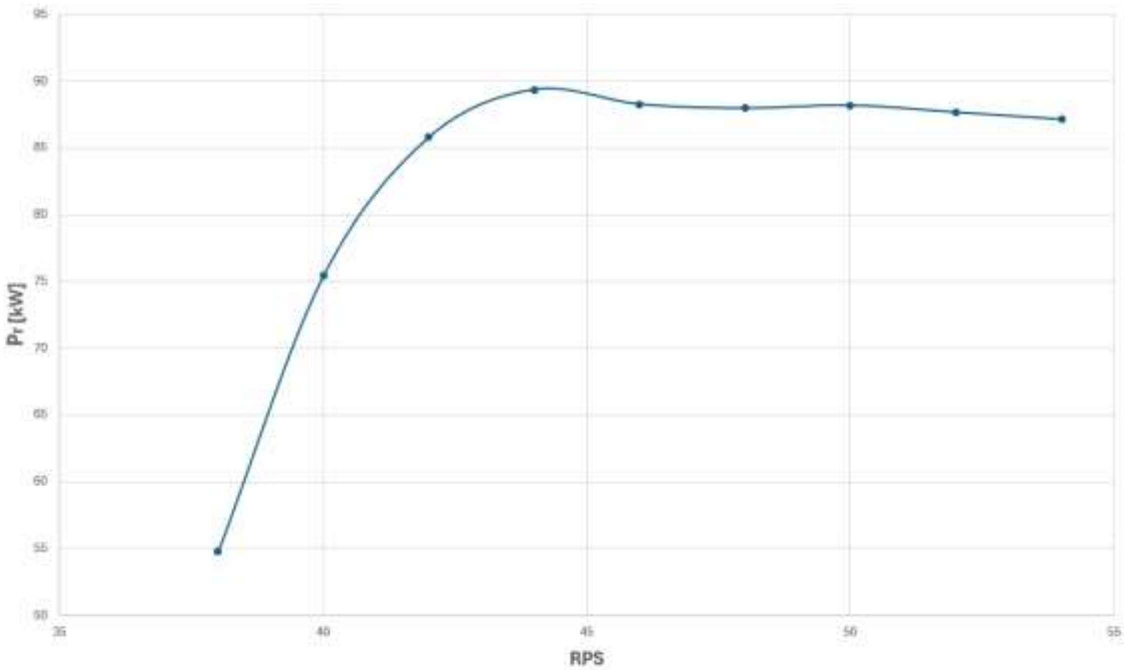

Fig. 13. Variation of available power of the engine-propeller system as a function of propeller rotational speed

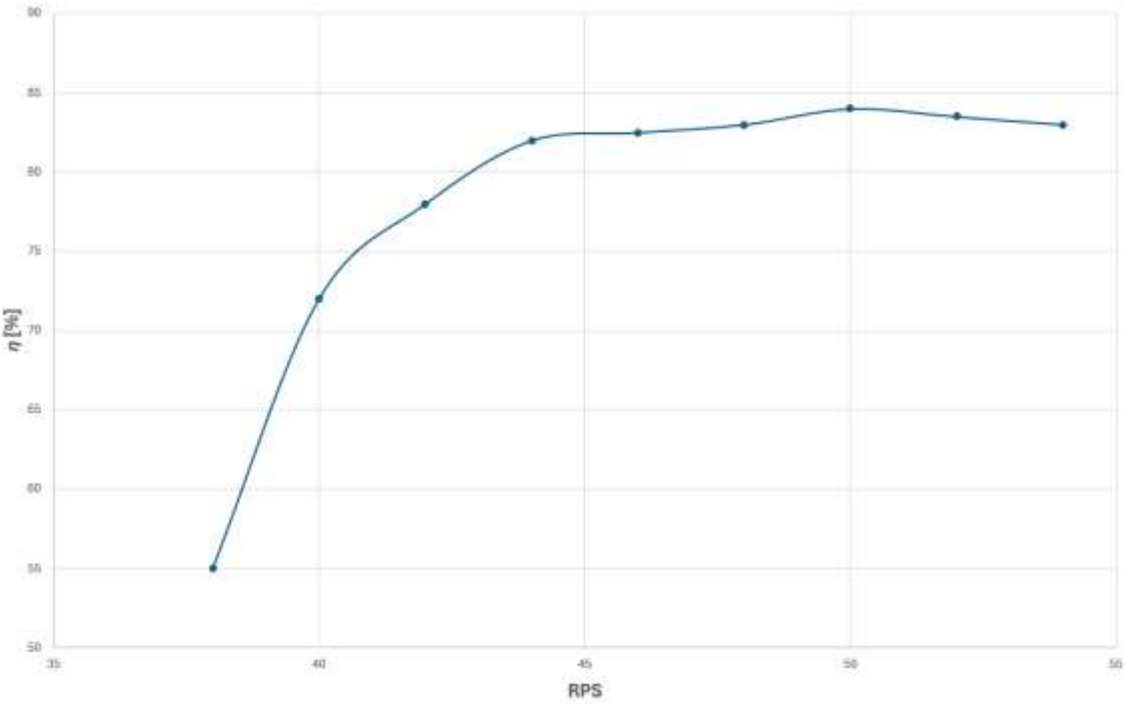

Fig. 14. Efficiency of the engine-propeller system as a function of propeller rotational speed

Based on the presented characteristics, relationships can be identified between propeller rotational speed, flight speed V, available power P_r, and the efficiency of the engine-propeller system η_p. With increasing rotational speed, a nearly linear increase in flight speed V is observed, indicating effective conversion of propulsion power into thrust T within the analyzed operating range.

At the same time, the available power characteristic P_r reaches a maximum in the mid-range of rotational speeds and then stabilizes, suggesting the achievement of an optimal operating point of the propulsion system. A similar trend is observed for efficiency η_p, which increases with rotational speed, reaches a maximum in a similar range, and then shows a tendency to stabilize or slightly decrease. This indicates that further increases in rotational speed do not result in a proportional increase in efficiency but only lead to increased system loads.

From an operational perspective, this indicates the existence of an optimal operating range of the propeller, in which the highest efficiency and a favorable ratio of generated thrust T to consumed power are achieved. Operation outside this range leads to reduced energy efficiency and increased aerodynamic losses, which is of direct importance in the selection of propulsion system parameters and its control in different phases of flight.

6. SUMMARY

The conducted analysis of the proposed algorithmic approach to determining geometric and aerodynamic parameters for propeller selection can be implemented in a universal manner, regardless of the type of propulsion unit used, provided that torque and power characteristics are employed as the primary input data. The applied algorithm enables an unambiguous determination of propeller operating parameters while maintaining the same geometry, which allows for direct comparison of different propulsion configurations.

From the perspective of propeller selection, kinematic constraints are of key importance, in particular the maximum allowable blade tip speed. This limitation directly determines the maximum propeller diameter and constitutes a primary design condition, independent of engine characteristics.

The study has shown that the selection of propeller diameter and blade setting angle is a compromise problem, in which the maximization of aerodynamic efficiency η_p must be considered together with the available power P_r and the operating conditions of the propulsion system. The highest propeller efficiency does not always correspond to the optimal operating point of the entire engine-propeller system.

The proposed procedure allows for the determination of propulsion system operating points and their analysis as a function of rotational speed, which constitutes an important tool in the design and selection of propulsion systems in light and unmanned aviation. Propeller selection should be treated as a problem of matching characteristics rather than designing geometry, while the presented procedure is theoretical in nature and is based on simplified models that, under real operating conditions, may lead to different results due to the influence of higher-order aerodynamic phenomena, interactions with the airframe, and flow unsteadiness.

Nomenclature

c – chord length [m],
C_p – power coefficient [–].
D – propeller diameter [m],
H_a – aerodynamic pitch [–],
H_g – geometric pitch [m],
J – advance ratio [–],
M_p – torque on the motor shaft [Nm],
P – engine power [kW],
P_p – power absorbed by the propeller [W],
P_r – available power [W],
R – propeller radius [m],
RPS – propeller rotational speed [1/s],
s – propeller slip [%],
T – thrust force [N],
V – flight speed [m/s],
V_{ad} – maximum propeller speed defined by safety factor [m/s],
V_∞ – free-stream airflow velocity vector [m/s],
V_s – slipstream velocity vector [m/s],
V_t – resultant airflow velocity vector [m/s],
V_{tip} – blade tip speed [m/s],
α – blade angle of attack [deg],
η_p – propeller efficiency [–],
θ – blade setting angle [deg],
ρ – air density [kg/m³],
Ω – propeller angular velocity vector [rad/s].

References

1. Buermann D., E. Hartman. 1939. *The aerodynamic characteristics of six full-scale propellers having different airfoil sections*.
2. Bukowski J., W. Łucjanek. 1986. *Propeller Drive: Theory and Design*. Warsaw: Publishing House of the Ministry of National Defense.
3. Alshahrani A. 2020. „Analysis and initial optimization of the propeller design for small, hybrid-electric propeller aircraft". Master's thesis, Stockholm.
4. MacNeill R., D. Verstraete. 2006. *Propeller optimisation for an electrically-powered tactical UAS*. The University of Sydney.
5. Reyner C., C. Lee, D. Kim, R. P. Liem. *Mission-based optimal propeller selection for VTOL SUAV configuration*. The Hong Kong University of Science and Technology; École Nationale de l'Aviation Civile.
6. Slavik S., J. Klesa. *Propeller selection by means of Pareto optimal sets applied to flight performance*. Czech Technical University.
7. Gur O., J. Feldman. „Engine-propeller matching". Israel Aerospace Industries.
8. EMRAX d.o.o. EMRAX 348 Technical Datasheet. Available at: https://emrax.com/e-motors/emrax-348/.
9. Răducanu G., R.-M. Dincă, et al. 2017. „Airplane propellers aerodynamic design and performances analysis". *Review of the Air Force Academy* 15(1): Article 12.
10. Adebimpe S. O. 2023. „Propeller aerodynamic design and optimization". *Preprints.org*. DOI: https://doi.org/10.20944/preprints202310.0418.v1.
11. Oliveira N. L., A.C. de C. Lemonge, P.H. Hallak, K. Kyprianidis, S. Vouros, M.A. Rendón. 2025. „Propeller design optimization and an evaluation of variable rotational speed flight operation under structural vibration constraints". *Machines* 13(6): 490. DOI: https://doi.org/10.3390/machines13060490.
12. Zheng F., W. Wang, S. Li, J. Zhang. 2015. „Matching characteristics of propeller and engine of fuel-powered quadrotor aircraft". *Proceedings of the 2015 2nd International Conference on Machinery, Materials Engineering, Chemical Engineering and Biotechnology*. DOI: https://doi.org/10.2991/mmeceb-15.2016.70.
13. McDonald R. A. 2015. „Modeling of electric motor driven propellers for conceptual aircraft design". *AIAA SciTech Forum*. DOI: https://doi.org/10.2514/6.2015-1676.
14. Filippone A. 2006. „Aerodynamics of propellers". *Progress in Aerospace Sciences* 42(5-6): 333-364. DOI: https://doi.org/10.1016/j.paerosci.2006.10.001.
15. Zenowicz P., W. Skarka. 2021. „Analysis and optimization of the propeller shape for a stratospheric drone research platform". *Advances in Transdisciplinary Engineering* 16: 147-156. DOI: https://doi.org/10.3233/ATDE210126.
16. Kim H., S. Park, J. Lee. 2023. „Development of an acoustic fault diagnosis system for UAV propeller blades". *CEAS Aeronautical Journal* 15: 881-893.
17. Hoffmann W., M. Żokowski. 2020. „Optimization of propeller aeroacoustics using genetic algorithms". *Science for Defence and Environment* 4(2): 45-58.
18. Zhang J., W. Li, L. Ren. 2024. „On minimum power flight formations of lifting propellers". *Aerospace Science and Technology* 149: 109150.
19. Chen Y., P. Li, X. Hu. 2024. „Helicopter rotor in a propeller slipstream". *Aerospace Science and Technology* 150: 109341.
20. Wei H., Z. Zhang, F. Zhou. 2024. „Wing-propeller aerodynamic interaction". *Aerospace Science and Technology* 151.

21. Wang L., X. Liu, Q. Zhang. 2024. „Optimization framework for high-altitude propellers". *Aerospace Science and Technology* 153. DOI: https://doi.org/10.3390/aerospace11110906.
22. Zanotti A., A. Velo, C. Pepe, A. Savino, D. Grassi, L. Riccobene. 2024. „Aerodynamic interaction between tandem propellers in eVTOL transition flight configurations". *Aerospace Science and Technology* 147: 109017. DOI: https://doi.org/10.1016/j.ast.2024.109017.
23. Biczyski M., R. Sehab, J. F. Whidborne, G. Krebs, P. Luk. 2020. „Multirotor sizing methodology with flight time estimation". *Journal of Advanced Transportation* 2020: Article 9689604. DOI: https://doi.org/10.1155/2020/9689604.
24. Podsędkowski M., D. Obidowski, M. Lipian. 2025. „Enhancing drone propellers: Practical insights from BEM-based pitch optimization". *Aerospace Science and Technology* 163: 110332. DOI: https://doi.org/10.1016/j.ast.2025.110332.
25. Gao M., W. Guo, J. Sun, Y. Huang, Y. Cai. 2026. „Aerodynamic optimization design of propellers for multi-rotor unmanned aerial vehicles based on NSGA-II". In: *Advances in Construction Machinery and Vehicle Engineering*. Springer. DOI: https://doi.org/10.1007/978-981-96-5527-4_65.

Received 23.03.2026; accepted in revised form 02.06.2026